2014

Modelling and Simulation of the Dynamics of Cross Vane Expander-Compressor Unit for Vapour Compression Cycle

Ken Shaun Yap
Nanyang Technological University, Singapore, Singapore / TUM CREATE, ksyap2@e.ntu.edu.sg

Kim Tiow Ooi
Nanyang Technological University, Singapore, Singapore, mktooi@ntu.edu.sg

Anutosh Chakraborty
Nanyang Technological University, Singapore, Singapore, AChakraborty@ntu.edu.sg

Modelling and Simulation of the Dynamics of Cross Vane Expander-Compressor Unit for Vapour Compression Cycle

Ken Shaun YAP[1,2a]*, Kim Tiow OOI[1b], Anutosh CHAKRABORTY[1c]

[1] School of Mechanical and Aerospace Engineering, Nanyang Technological University, 50 Nanyang Avenue, Singapore 639798.
[2]TUM CREATE (Technische Universität München - Campus for Research Excellence And Technological Enterprise), 1 CREATE Way, #10-02, CREATE Tower, Singapore 138602.

[a]Phone: +65 6592 3755, email: ksyap2@e.ntu.edu.sg
[b]Phone: +65 6790 5511, e-mail: mktooi@ntu.edu.sg
[c]Phone: +65 6790 4222, email: achakraborty@ntu.edu.sg

* Corresponding Author

ABSTRACT

The Cross Vane mechanism was recently invented and employed in the design and development of an expander-compressor unit, named Cross Vane expander-compressor or CVEC in short. This device replaces the compressor and expansion valve of a conventional vapour compression cycle, and improves the energy efficiency of the system. Theoretical models which include geometrical, thermodynamics, mass flow, as well as mechanical loss models are developed to characterize the performance of CVEC. Numerical simulation was performed, and the results show that the device is capable of reducing the energy consumption and the peak instantaneous power requirement of the refrigeration system. Energy saving and peak instantaneous power reduction of up to 18.0% and 3.8% respectively is achievable with the introduction of CVEC. In addition, due to its unique rotating cylinder design the mechanical losses in CVEC are relatively low. Its mechanical efficiency is calculated to be up to 96.5%.

1. INTRODUCTION

A new type of expander-compressor unit called CVEC was recently introduced to replace the compressor and expansion valve in the conventional refrigeration systems in order to improve the energy efficiency of the system. The design and assembly, as well as the working principle of the CVEC has been introduced and explained in detail in the first paper entitled: Introduction of the Novel Cross Vane Expander-Compressor Unit for Vapour Compression Cycle (Yap *et al.*, 2014), which will be published in the same proceedings. The novel mechanism combines the function of compressor and expander into a single integrated unit as opposed to other expander-compressor systems, whereby a separated compressor is directly coupled to a separated expander using a connecting shaft (Kim *et al.*, 2008, Kohsokabe *et al.*, 2006, Kovacevic *et al.*, 2006). This makes CVEC smaller in size, compact, and highly energy efficient.

In its basic form, the CVEC consists of 3 major components: the outer cylinder-vane-shaft assembly, the inner cylinder, and the split bush as shown in Figure 1. The vane is rigidly fixed to the shaft and the outer cylinder as one assembly. The outer cylinder-vane-shaft assembly is then assembled eccentrically with the inner cylinder. As a result, the suction and discharge chamber of the expander, and the suction and compression chamber of the compressor are formed.

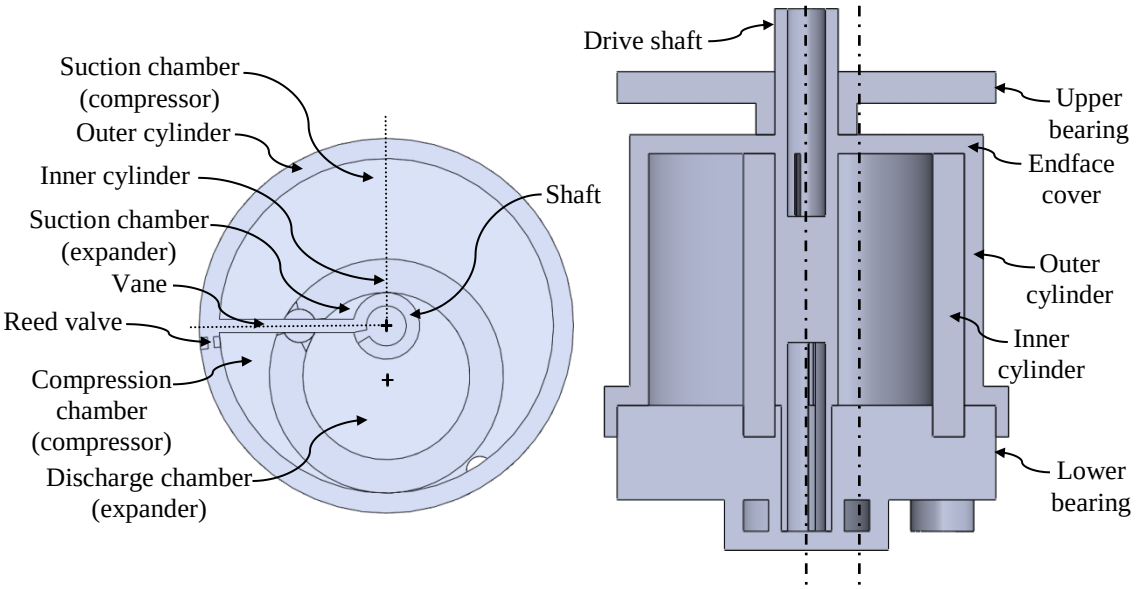

Figure 1: Front and side sectional view of CVEC

The working principle of CVEC is illustrated in Figure 2. The expander is located at the inner chambers and the compressor is located at the outer chambers. During operation, the compressor work is supported by the prime mover (such as an electric motor) and also the expansion work recovered in the expander. Therefore, lesser work is required from the prime mover and the efficiency of the refrigeration system is increased.

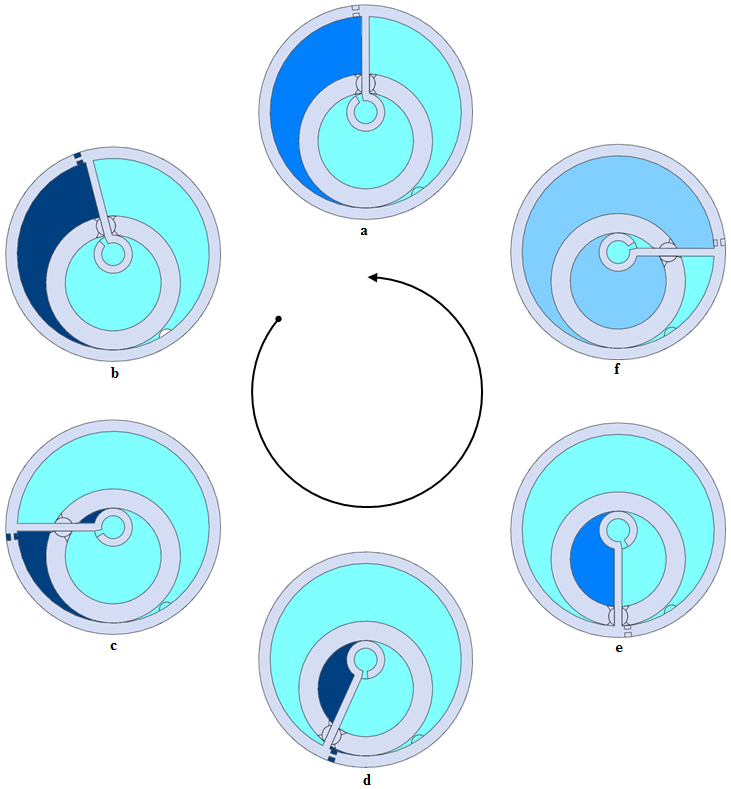

Figure 2: The working principle of CVEC

In this paper, theoretical models i.e. geometrical, thermodynamics, mass flow, and mechanical loss models, which describe the performance of CVEC, will be presented. The numerical approach to these models will then be explained, and the operating specifications and main dimensions of CVEC are given. The simulation results are then presented and discussed.

2. THEORETICAL MODELLING

2.1 Geometrical Models

In general, the variation in thermodynamics properties of the working fluid is a consequence of volume variation. Thus, the geometrical models can be regarded as prime driver for the entire performance simulation of the expander-compressor unit.

The suction chamber volume, V_{escv} and discharge chamber volume, V_{edcv} of the expander are derived as shown in Equations 1 and 2.

$$V_{escv} = \frac{1}{2}[{r_{ic}}^2\theta_2 - {r_r}^2\theta_1 - (l_i + r_s)(r_{ic} - r_s)sin\theta_1]l_{eps} \tag{1}$$

$$V_{edcv} = \pi({r_{ic}}^2 - {r_s}^2)l_{eps} - \frac{1}{2}[{r_{ic}}^2\theta_2 - {r_r}^2\theta_1 - (l_i + r_s)(r_{ic} - r_s)sin\theta_1]l_{eps} \tag{2}$$

where

$$l_i = -(r_{ic} - r_s)cos\theta_1 - r_s + \sqrt{{r_{ic}}^2 - (r_{ic} - r_s)^2 sin^2\theta_1} \tag{3}$$

The suction chamber volume, V_{cscv} and discharge chamber volume, V_{cdcv} of the compressor are derived as shown in Equations 4 and 5.

$$V_{cscv} = \frac{1}{2}\left[{r_{oc}}^2(\theta_1 - \pi) + (\pi - \theta_2)(r_{ic} + t_{ic})^2 + \left(l_{i+t_{ic}} + r_s\right)(r_{ic} - r_s)sin\theta_1 - \left(l_v - l_{i+t_{ic}}\right)w_v\right]l_{eps} \tag{4}$$

$$V_{cdcv} = \pi({r_{oc}}^2 - (r_{ic} + t_{ic})^2)l_{eps} - V_{cscv} \tag{5}$$

where

$$l_{i+t_{ic}} = -(r_{ic} - r_s)cos\theta_1 - r_s + \sqrt{(r_{ic} + t_{ic})^2 - (r_{ic} - r_s)^2 sin^2\theta_1} \tag{6}$$

$$l_o = l_v - l_{i+t_{ic}} \tag{7}$$

2.2 Thermodynamics and Mass Flow Models

The working chamber of CVEC is made up of the suction and compression chambers of the compressor, as well as the suction and discharge chambers of the expander. During operation, the volumes of these working chambers change, and as a result, the fluid properties such as pressure, temperature, and density in each of these working chambers vary. An energy rate balance for a control volume based on the Law of Conservation of Energy is given in Equation 8. The equation assumes that gas properties are instantaneously propagated throughout the whole working chamber, or in other words, they are uniform and have no spatial variation.

$$\frac{dE_{cv}}{dt} = \dot{Q}_{cv} - \dot{W}_{cv} + \sum_i \dot{m}_i\left(h_i + \frac{{\mathrm{v}_i}^2}{2} + gz_i\right) - \sum_o \dot{m}_o\left(h_o + \frac{{\mathrm{v}_o}^2}{2} + gz_o\right) \tag{8}$$

The second term on the right hand side of the equation represents work done due to volumetric change, and can be expressed as

$$\frac{dW_{cv}}{dt} = p_{cv}\frac{dV_{cv}}{dt} \tag{9}$$

In addition, the total energy of the control volume comprises the internal energy, kinetic energy, and gravitational potential energy. It can be expressed specifically as

$$E_{cv} = m_{cv}\left(u_{cv} + \frac{{\mathrm{v}_{cv}}^2}{2} + gz_{cv}\right) \tag{10}$$

Therefore, substituting Equations 9 and 10 into Equation 8, and using the product rule and ignoring all the potential energy as well as kinetic energy components of the control volume and inlet/outlet flow, we have

$$m_{cv}\frac{du_{cv}}{dt}+u_{cv}\frac{dm_{cv}}{dt}=\frac{dQ_{cv}}{dt}-p_{cv}\frac{dV_{cv}}{dt}+\sum_{i}\frac{dm_i}{dt}h_i-\sum_{o}\frac{dm_o}{dt}h_o \tag{11}$$

By the Law of Conservation of Mass, the net rate of change of mass in the control volume, $\dot{m}_{cv}$ can be written as

$$\frac{dm_{cv}}{dt}=\sum_{i}\frac{dm_i}{dt}-\sum_{o}\frac{dm_o}{dt} \tag{12}$$

The mass flow rate through the suction port, $\dot{m}_i$ and discharge port, $\dot{m}_o$ of the compressor and expander is analysed as a one dimensional flow through an orifice. By applying the Law of Conservation of Energy to the orifice model and assuming isentropic flow, we have

$$\frac{dm_{i/o}}{dt}=C_d\rho_{2s}A_{i/o}\sqrt{2\left(h_i-h_{o,s}\right)} \tag{13}$$

2.3 Mechanical Loss Models

The frictional power losses at the various contact regions of the expander-compressor unit are derived and presented in this section. Major frictional losses include: vane side friction, split bush friction, and the various endface friction.

Vane side friction occurs when the vane slides along the slot of the split bush during operation. The power loss is derived as shown in Equation 14.

$$P_{vs}=\frac{dl_v}{dt}\mu_{vs}\left(\frac{I_{ic}\alpha_2}{r_{ic}+\frac{t_{ic}}{2}}\right)cos\gamma \tag{14}$$

where

$$\gamma=\begin{cases}cos^{-1}\left(\dfrac{\left(r_{ic}+\frac{t_{ic}}{2}\right)^2+\left(r_s+l_{i+t_{ic}/2}\right)^2-(r_{ic}-r_s)^2}{2\left(r_{ic}+\frac{t_{ic}}{2}\right)\left(r_s+l_{i+t_{ic}/2}\right)}\right);\ 0\le\theta_1\le\pi\\ -cos^{-1}\left(\dfrac{\left(r_{ic}+\frac{t_{ic}}{2}\right)^2+\left(r_s+l_{i+t_{ic}/2}\right)^2-(r_{ic}-r_s)^2}{2\left(r_{ic}+\frac{t_{ic}}{2}\right)\left(r_s+l_{i+t_{ic}/2}\right)}\right);\ \pi\le\theta_1\le2\pi\end{cases} \tag{15}$$

Split bush friction occurs due to the swivelling motion of the split bush about the hinge joint located at the inner cylinder during operation. The power loss is derived as shown in Equation 16.

$$P_{sb}=(\omega_1-\omega_2)r_{sb}\mu_{sb}\sqrt{\left(\mu_{vs}\left(\frac{I_{ic}\alpha_2}{r_{ic}+\frac{t_{ic}}{2}}\right)cos\gamma\right)^2+\left(\left(\frac{I_{ic}\alpha_2}{r_{ic}+\frac{t_{ic}}{2}}\right)cos\gamma\right)^2} \tag{16}$$

The frictional power loss between the lower endface of the inner cylinder and the surface of the lower bearing is derived as shown in Equation 17.

$$P_{ic,lb}=\frac{\pi{\omega_2}^2\mu_{iclb}[(r_{ic}+t_{ic})^4-{r_{ic}}^4]}{2\delta_{iclb}} \tag{17}$$

The frictional power loss between the lower endface of the outer cylinder and the surface of the lower bearing is derived as shown in Equation 18.

$$P_{oc,lb} = \frac{\pi {\omega_1}^2 \mu_{oclb}[(r_{oc} + t_{oc})^4 - {r_{oc}}^4]}{2\delta_{oclb}} \quad (18)$$

The frictional power loss between the upper endface of the inner cylinder and outer cylinder is derived as shown in Equation 19.

$$P_{ic,oc} = -\frac{\mu_{icoc}\pi {\omega_1}^2 e^2}{\delta_{icoc}}((r_{ic} + t_{ic})^2 - {r_{ic}}^2) - \frac{\mu_{icoc}\pi(\omega_2 - \omega_1)^2}{2\delta_{icoc}}((r_{ic} + t_{ic})^4 - {r_{ic}}^4) \quad (19)$$

3. NUMERICAL ANALYSIS

The mathematical models that were presented earlier were solved numerically with MATLAB. In particular, the geometrical, thermodynamics and mass flow model were integrated simultaneously using the 4th order Runge-Kutta method, whereby in each integration step, the instantaneous thermodynamics properties of the working fluid are provided by NIST database using REFPROP routine (Lemmon *et al.*, 2010). Prior to the numerical simulation, the assumptions adopted in the analysis are: perfect sealing, adiabatic condition, instantaneous valve response, and constant shaft angular velocity.

The operating specifications, main geometrical dimensions and physical parameters of the expander-compressor unit are tabulated as shown in Tables 1 and 2.

Table 1: Operating specifications

Operating Specifications	
Working fluid	R-134a
Degree of superheat	27.8°C
Saturated temperature of condenser	54.4°C
Saturated temperature of evaporator	7.2°C
Operational speed	3000 rev/min
Cooling load	5275 W

Table 2: Geometrical dimensions and physical parameters of CVEC

Main Dimensions	
Radius of shaft, r_s	5.0 mm
Radius of inner cylinder, r_{ic}	10.0 mm
Radius of outer cylinder, r_{oc}	28.0 mm
Thickness of inner cylinder, t_{ic}	13.0 mm
Thickness of outer cylinder, t_{oc}	2.0 mm
Length of vane, l_v	23.0 mm
Length of expander-compressor unit, l_{eps}	52.0 mm
Capacity of compressor	41.9 cm^3
Capacity of expander	12.2 cm^3

4. RESULTS AND DISCUSSIONS

The pressure-volume (pV) diagram of the expander is shown in Figure 3. The suction process is so short that the expansion process happens almost immediately, and the pressure of the fluid drops to that of around discharge pressure. During the discharge process, a curvilinear graph that curves upwards is obtained. This also indicates that discharge flow initially cannot keep up with the expander movement, until a point whereby the pressure difference is sufficiently large enough to create high flow rate to decrease the pressure.

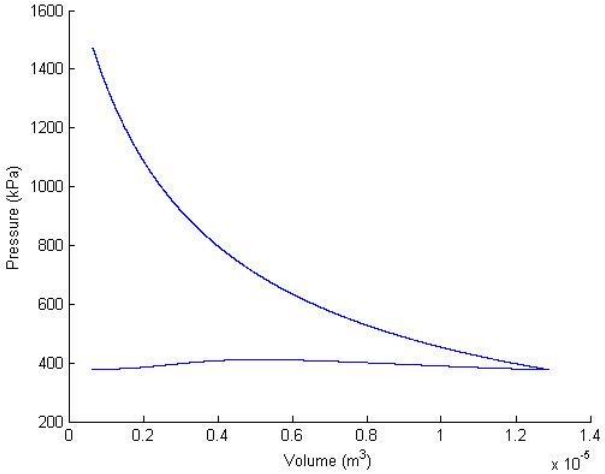

Figure 3: pV diagram of expander

The pV diagram of compressor is shown in Figure 4. During the suction process, the pressure of working fluid drops below that of the suction pressure, and then increases again at around the halfway point. The curvilinear behaviour indicates that suction flow initially cannot keep up with the compressor movement, until a point whereby the pressure difference is sufficiently large enough to create high flow rate to increase the pressure. During the compression process, the fluid is compressed up to around the discharge pressure. At this time, the discharge valve opens so that fluid flows out through the discharge port. However, due to the small opening area of the discharge port, the discharge flow cannot keep up with the speed of compressor. This results in a pressure build-up in the compression chamber, until a point whereby the pressure difference is large enough to produce high flow rate to reduce the pressure.

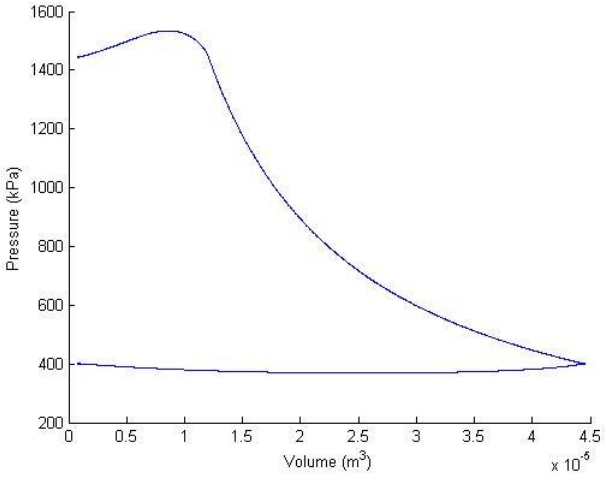

Figure 4: pV diagram of compressor

To understand the behaviour of the expander-compressor unit in a greater detail, the instantaneous power is broken into its constituent powers, i.e. the compressor power, expander power, and total frictional power loss, as shown in Figure 5. From the figure, the graphs of compressor power and expander power show that the compressor and expander cycles are 180º out of phase from each other and that they are of opposite signs. The average power of the compressor, expander, and total frictional loss are calculated to be 1107.5 W, -174.5 W, and 34.0 W, respectively. The total frictional loss CVEC is comparatively small due to its unique rotating cylinder design. As a result, a mechanical efficiency of 96.5% could be obtained.

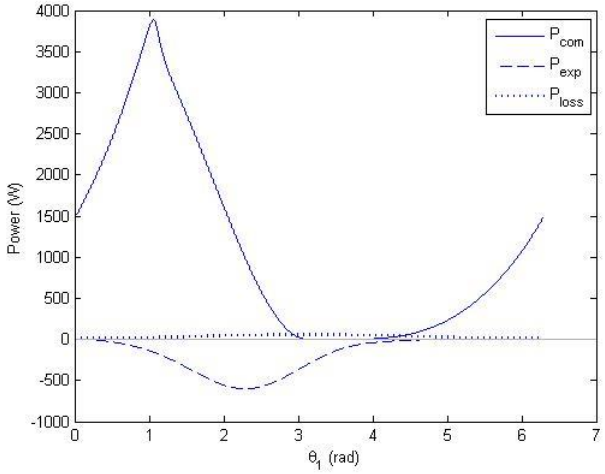

Figure 5: Instantaneous power constituents of CVEC

Figure 6 shows the instantaneous power of a refrigeration system with and without CVEC. It can be observed that the instantaneous power with CVEC is always below that of the one without CVEC. This shows that the expansion power recovered from the expander can be utilised to partially drive the compressor and reduce the energy consumption of the system. An energy saving of up to 18.0% could be achieved. In addition, the expansion power recovered from the expander also results in the decrease of peak instantaneous power of the system from 3955.1 W to 3802.8 W, i.e. a reduction of 3.8%.

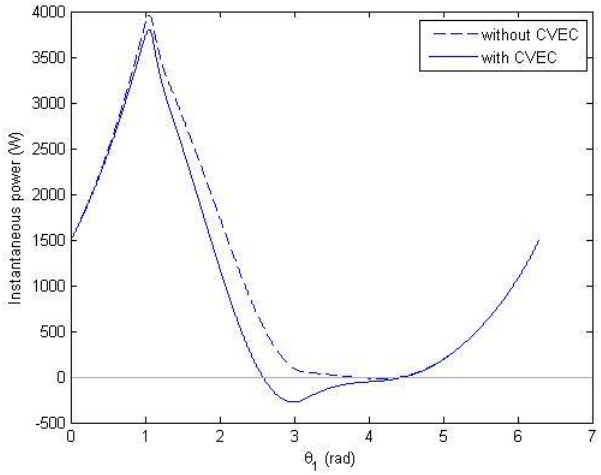

Figure 6: Instantaneous power with and without CVEC

5. CONCLUSIONS

In this paper, the theoretical work which describes the performance of CVEC such as geometrical, thermodynamics, mass flow, and mechanical loss models are presented. Numerical simulation was performed using MATLAB and REFPROP, and the assumptions are: homogenous properties in the control volume, quasi equilibrium, perfect sealing, adiabatic condition, instantaneous valve response, and constant speed. The simulation was conducted using R-134a as the working fluid, cooling load of 5275W, operational speed of 3000 rpm, saturated temperature of condenser at 54.4ºC and saturated temperature of evaporator at 7.2ºC. The capacity of the compressor and expander is 41.9 cm^3 and 12.2 cm^3 respectively, whereby the outer cylinder radius is 28.0 mm and the length of the expander-compressor unit is 52.0 mm. The geometrical model produces volume variation of the working chambers, which is used to compute the pressure and temperature of the working fluid in the thermodynamics and mass flow models. Mechanical losses of the expander-compressor unit are then calculated and the instantaneous power of the machine is obtained. The results were presented and discussed in terms of mechanical efficiency of the expander-compressor unit and the energy saving of the system. It is found that energy saving and peak instantaneous power reduction of up to 18.0% and 3.8%

respectively is achievable with the introduction of CVEC, and its mechanical efficiency is calculated to be up to 96.5%.

NOMENCLATURE

A	area	(m^2)
C_d	coefficient of discharge	(-)
e	eccentricity	(m)
E	energy	(J)
g	acceleration of free fall	(m/s^2)
h	specific enthalpy	(J/kg)
I	moment of inertia	($kg \cdot m^2$)
l	length	(m)
m	mass	(kg)
p	pressure	(Pa)
P	power	(W)
Q	heat transfer	(J)
r	radius	(m)
t	time or thickness	(s or m)
u	Specific internal energy	(J/kg)
v	velocity	(m/s)
V	volume	(m^3)
w	width	(m)
W	work	(J)
z	height	(m)
θ	rotational angle	(rad)
ω	angular velocity	(rad/s)
α	angular acceleration	(rad/s^2)
γ	angle subtended by shaft and inner cylinder	(rad)
δ	clearance	(m)
μ	dynamic viscosity or coefficient of friction	(Pa·s or -)
ρ	density	(kg/m^3)

Subscript

1	about shaft centre
2	about inner cylinder centre
cv	control volume
$cdcv$	compressor compression chamber
$cscv$	compressor suction chamber
$edcv$	expander discharge chamber
$escv$	expander suction chamber
eps	expander-compressor unit
i	inflow or inner
ic	inner cylinder
lb	lower bearing
o	outflow or outer
oc	outer cylinder
s	shaft or isentropic
sb	split bush
v	vane
vs	vane side

REFERENCES

Kim, H.J., Ahn, J.M., Cho, S.O., Cho, K.R., 2008, Numerical Simulation on Scroll Expander-compressor Unit for CO_2 Transcritical Cycle, *Appl. Therm. Eng.*, vol.28, no. 13, 1654-1661.

Kohsokabe, H., Funakoshi, S., Tojo, K., Nakayama, S., Kohno, K., Kurashige, K., 2006, Basic Operating Characteristics of CO_2 Refrigeration Cycles With Expander-Compressor Unit, *International Refrigeration and Air Conditioning Conference*, Purdue e-Pubs, R159.

Kovacevic, A., Stosic, N., Smith, I.K., 2006, Numerical Simulation of Combined Screw Compressor-expander Machines for Use in High Pressure Refrigeration Systems, *Simul. Model. Pract. Th.*, vol.14, no. 8, 1143-1154.

Lemmon, E.W., Huber, M.L., McLinden, M.O., 2010, *NIST Standard Reference Database 23: Reference Fluid Thermodynamic and Transport Properties-REFPROP*, Gaithersburg, National Institute of Standards and Technology.

Yap, K.S., Ooi, K.T., Chakraborty, A., 2014, Introduction of the Novel Cross Vane Expander-Compressor Unit for Vapour Compression Cycle, *International Refrigeration and Air Conditioning Conference*, Purdue e-Pubs, Paper no. 1129.